

Tunable colour emission from patterned porous silicon using ion beam writing

E.J. Teo ^{a,b,*}, M.B.H. Breese ^b, A.A. Bettiol ^b, F.J.T. Champeaux ^b,
T.L.S.L. Wijesinghe ^a, D.J. Blackwood ^a

^a Department of Materials Science and Engineering, National University of Singapore, 7 Engineering Drive 1, Singapore 117574, Singapore

^b Department of Physics, Centre for Ion Beam Applications, National University of Singapore, 2 Science Drive 3, Singapore 117542, Singapore

Available online 14 February 2007

Abstract

Combined ion beam irradiation and electrochemical etching of silicon has been used to pattern light emitting porous silicon. A highly focused beam of helium ions is made to scan across a 4 Ω cm resistivity silicon in a predefined manner. As the ion beam penetrates the sample, it induces lattice damage and increases the local resistivity of the material. This slows down the rate of porous silicon formation, so that a thinner porous layer is formed at the irradiated regions. In this work, the photoluminescence properties of the irradiated porous silicon are studied as a function of dose. The porous silicon is then removed to reveal the underlying irradiated structure. The decrease in thickness of porous silicon with dose is correlated with the observed change in photoluminescence properties.

© 2007 Elsevier B.V. All rights reserved.

PACS: 42.82.Cr; 61.80.Jh; 78.55.Mb; 78.67.Bf

Keywords: Light emitting porous silicon; Patterning; Ion irradiation; Photoluminescence

1. Introduction

Porous silicon is of interest due to its visible photoluminescence at room temperature and compatibility with standard microelectronic process. The ability to emit light at energies greater than the silicon bandgap of 1.1 eV is probably due to the quantum confinement effects produced by the low dimensionality of silicon skeleton after etching [1]. The light emitting properties of porous silicon can be varied by changing the etching current densities [2], oxidation [3] or photochemical etching [4,5]. In order to alter its light emission at micron scale, patterning techniques such as optical [6,7], electron [8] and soft lithography [9] are used to selectively quench or enhance light intensity. Ion beam

irradiation with 100–300 keV silicon [10,11] have been shown to affect the wavelength emission in addition to its intensity.

At the Centre for Ion Beam Applications Laboratory, National University of Singapore, the ultra-stable, high brightness Singletron™ accelerator is capable of producing protons and helium ions with energy up to 3.5 MV [12]. It has already been shown that high energy proton beam irradiation prior to electrochemical etching can be used to fabricate precise, three-dimensional microstructures in silicon [13–15] and GaAs [16]. In this work, we demonstrate that energetic hydrogen or helium ions can be used to produce controlled light emission from patterned porous silicon [17–19]. The advantage of using high energy ions over lower energy, heavier ions used in previous studies is that the range is much deeper and damage is 2–3 orders of magnitude lower. This provides greater control over the resultant PL emission due to the thicker damaged layer and reduced rate of damage with dose. We use this

* Corresponding author. Address: Department of Physics, Centre for Ion Beam Applications, National University of Singapore, 2 Science Drive 3, Singapore 117542, Singapore. Tel.: +65 65168743; fax: +65 67776126.
E-mail address: msetej@nus.edu.sg (E.J. Teo).

principle to produce patterned micron-sized areas of porous silicon with widely differing PL wavelengths and intensities on a single substrate.

2. Experimental procedures

Fig. 1 shows a schematic diagram of the fabrication process. The irradiation of the p-type silicon ($\sim 4 \Omega \text{ cm}$) was carried out using a nuclear microprobe [12,20]. A beam of 2 MeV helium ions, focused down to sub-micron resolution was used to selectively damage the silicon lattice. This was done by feeding the predefined pattern into the software *Ionscan* [21], which was used to control the scanning of the beam. Damage mechanism and its effects on the resistivity of the silicon are described in [15], based on earlier observations of MeV ion induced damage for Ion Beam Induced Charge Microscopy [22,23]. The dose at each region is determined by the amount of time the beam accumulates at the particular region, so by pausing the beam for different times at different regions, any pattern of localized damage can be built up. This buried layer of damage acts as an electrical barrier which slows down the rate of holes migrating to the surface during anodization. By varying the beam dose, porous silicon with variable thickness can be formed over the irradiated patterns.

After irradiation, the sample was then cleaned with diluted HF ($<10\%$) and electrical contact was made to the backside of the sample using In–Ga eutectic paint and copper wire. A thick layer of epoxy was applied to protect the electrical contact during etching. Subsequently, the sample was then etched electrochemically in a mixture of hydrofluoric acid, ethanol and water in the ratio of 1:2:1 at 100 mA/cm^2 for 5 min. Ethanol was added to reduce

the surface tension and thus surface roughness during bubble formation. After etching, the sample was then rinsed in ethanol and then in distilled water for about 5 min.

Photoluminescence (PL) spectroscopy was carried out at room temperature using a 405 nm diode laser. The laser light was focused onto the sample through a ME600 Nikon microscope with a $100\times$ objective. The PL signals were then detected with a charge-coupled device (CCD) Ocean Optics Spectrometer via an optical fiber. Most of the laser light had been cut off using a 495 nm long pass filter. All PL spectra had been corrected for system response. For PL imaging, the patterned porous silicon was illuminated using a UV lamp and the images were collected using a CCD camera. Scanning electron microscopy (SEM) was then used to study the underlying irradiated structure after porous silicon removal (Fig. 1(c)).

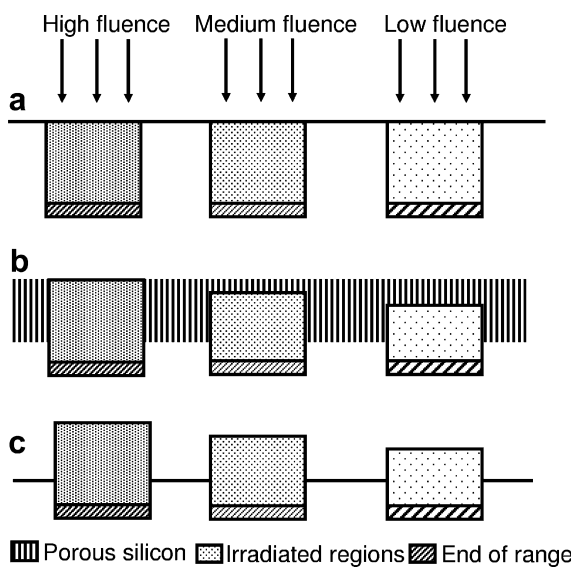


Fig. 1. Schematic diagram of the fabrication process. (a) Patterning of silicon using helium beam irradiation, followed by (b) electrochemical etching. (c) Porous silicon removal using potassium hydroxide (KOH) reveals the underlying structure.

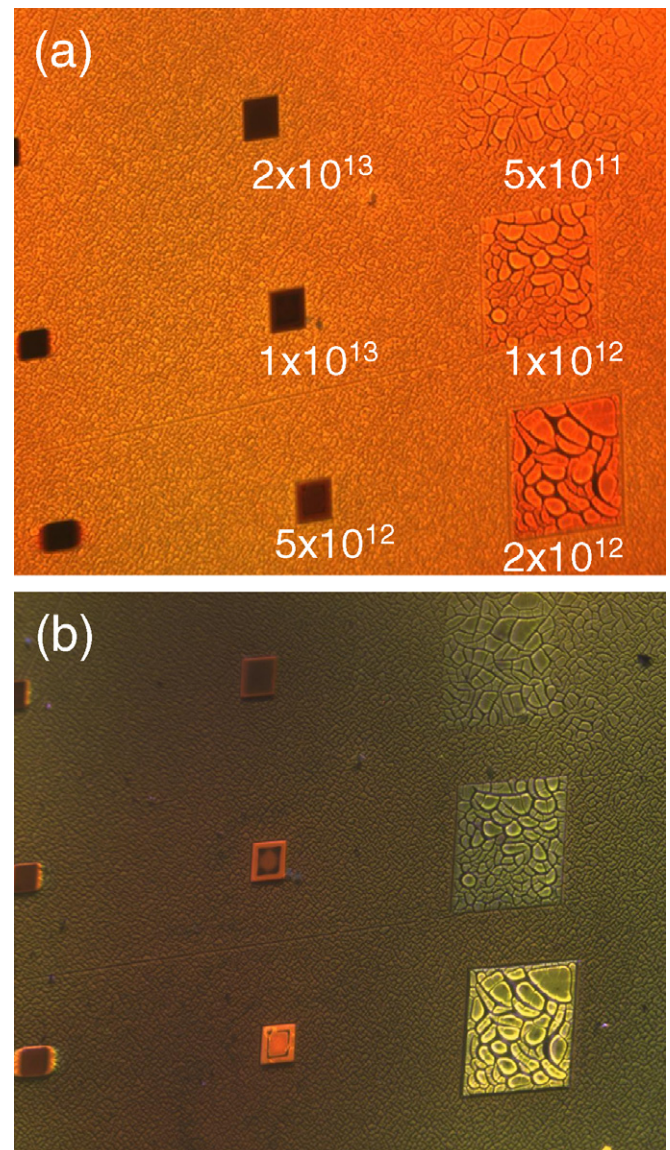


Fig. 2. (Colour online) PL image of the patterned porous silicon (a) immediately after etching and (b) after 20 days.

3. Results

A series of squares was irradiated with a range of doses from 5×10^{11} to $2 \times 10^{13} \text{ cm}^{-2}$. Fig. 2(a) shows the PL image of the patterned porous silicon immediately after etching. It is found that the unirradiated regions appear orange and the squares with doses of 5×10^{12} and $1 \times 10^{13} \text{ cm}^{-2}$ appear reddish in colour. Higher doses result in a much reduced light emission from the squares. By leaving the sample to age in a tightly sealed chamber for 20 days, the PL emission is slowly changed from orange to green (see Fig. 2(b)). The progressive slow oxidation process reduces the size of the nanocrystals contained in the porous silicon, causing the background to turn green. The irradiated squares show similar blue-shift with time.

It also becomes more apparent that the wavelength emission of the irradiated squares red-shifts with dose, resulting in multi-colour emission of green, yellow, orange to red on a single substrate.

Fig. 3 shows the PL spectra collected from the irradiated squares in Fig. 2(b). The peak wavelength is red-shifted from 595 nm for a dose of $1 \times 10^{12} \text{ cm}^{-2}$ to 656 nm for a dose of $1 \times 10^{13} \text{ cm}^{-2}$. For doses higher than $1 \times 10^{13} \text{ cm}^{-2}$, the intensity of the PL emission becomes too low to be detected by the PL system. By careful control of the dose of the beam, it is possible to tune the wavelength emission of the patterned porous silicon.

Results show that significant change in PL emission can only be observed for a dose range of 5×10^{11} – $1 \times 10^{13} \text{ cm}^{-2}$. For doses lower than $5 \times 10^{11} \text{ cm}^{-2}$, the PL emission

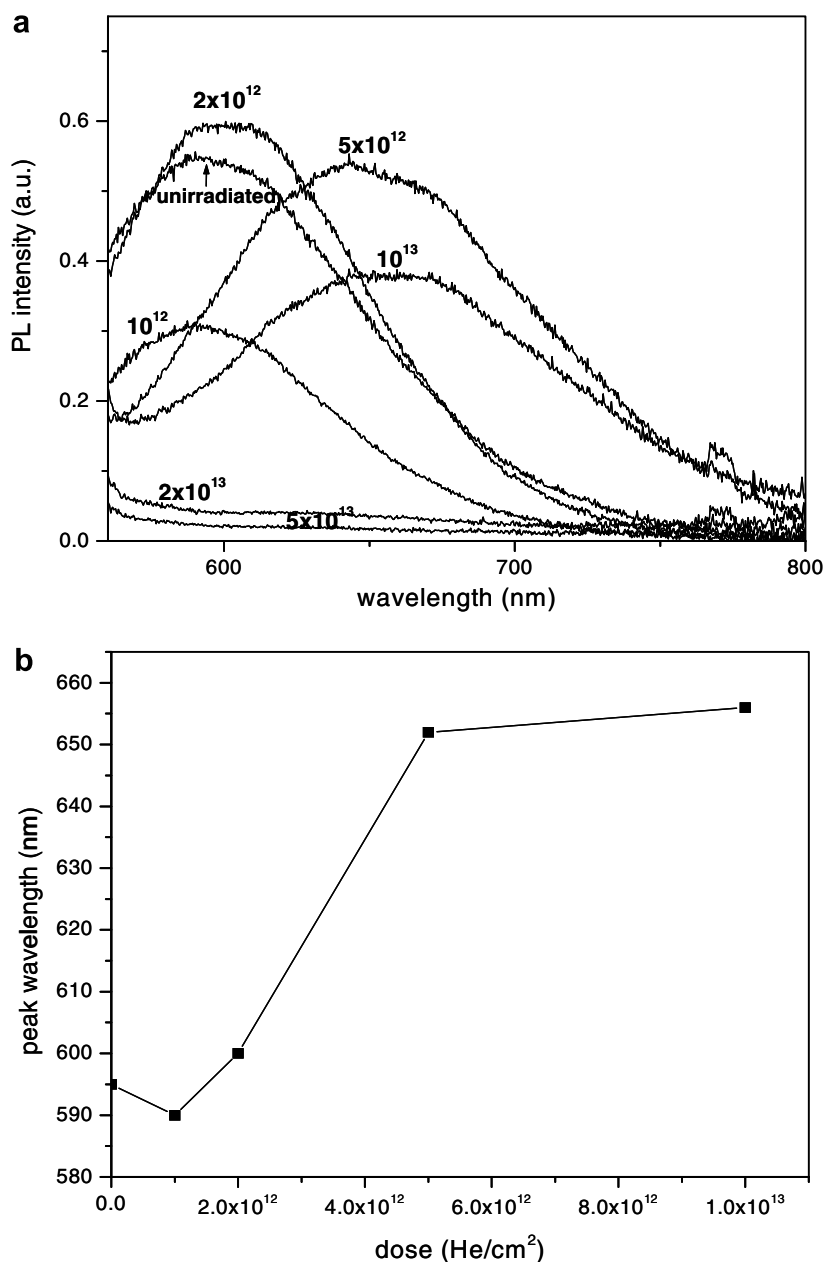


Fig. 3. (a) PL spectra of the irradiated regions after 20 days and (b) plot of peak wavelength versus dose.

is remains unaltered by the ion irradiation. For doses higher than $1 \times 10^{13} \text{ cm}^{-2}$, the intensity is almost completely quenched. The porous silicon layer is removed with potassium hydroxide to reveal the underlying irradiated structures (see Fig. 1(c)). Fig. 4 shows SEM of the irradiated

structures with different doses. At dose of $5 \times 10^{11} \text{ cm}^{-2}$, the beam damage of the beam is too low to induce a significant change in the etch rate of the porous silicon, resulting in negligible change in structure height. At a dose of $2 \times 10^{12} \text{ cm}^{-2}$, the structure height starts to

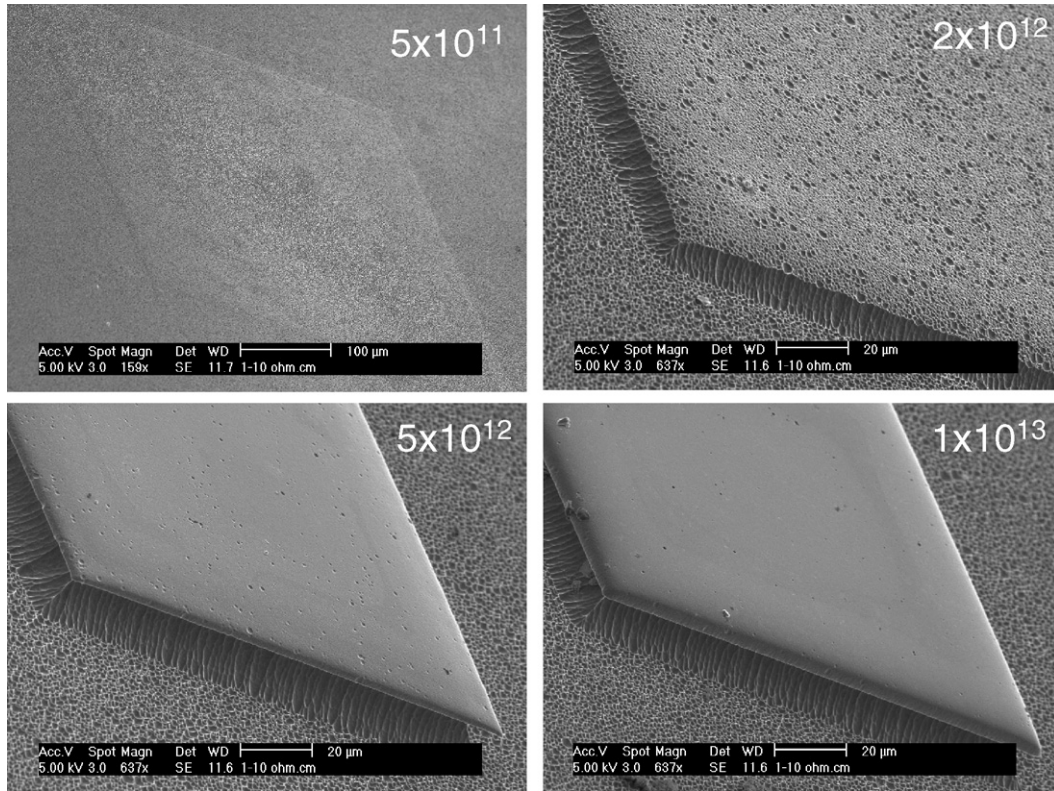


Fig. 4. SEM images of the irradiated squares with the porous silicon layer removed.

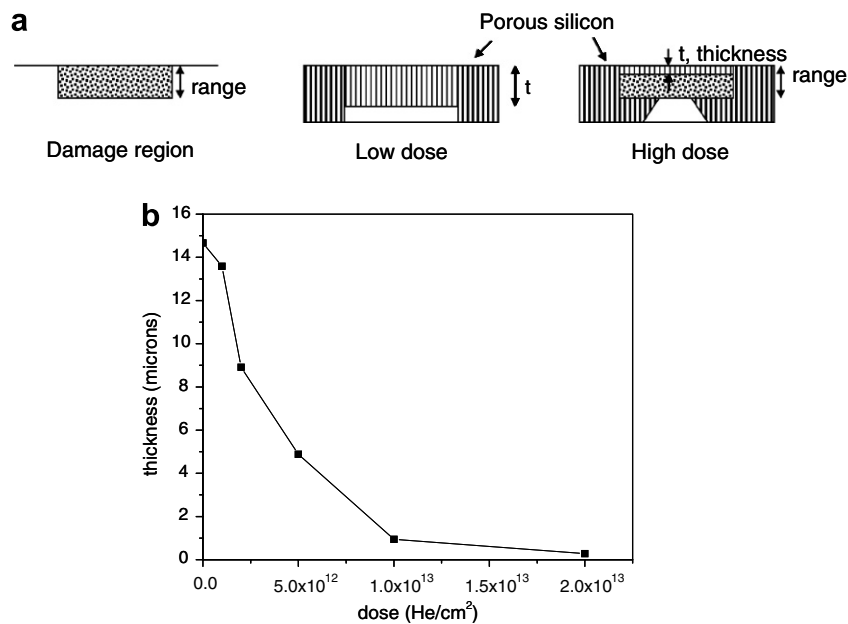


Fig. 5. (a) Schematic diagram of the structures with low and high dose irradiation as etching occurs beyond the end of range. (b) Plot of thickness of porous silicon versus dose.

increase, indicating a slower rate of porous silicon formation. At doses of 5×10^{12} and $1 \times 10^{13} \text{ cm}^{-2}$, undercutting of the irradiated structure can be observed as the porous silicon is etched beyond the end of range of 2 MeV He. The etch rate is almost reduced to zero for doses higher than $1 \times 10^{13} \text{ cm}^{-2}$.

The etching process can be divided into two different dose regimes (see Fig. 5(a)). Under such etching conditions, the layer of porous silicon formed is about $14.6 \mu\text{m}$. This depth is thicker than the range of 2 MeV He of $7.3 \mu\text{m}$. In the case of doses $2 \times 10^{12} \text{ cm}^{-2}$ and below, the etch rate is only slightly slower than the unirradiated regions, and the porous silicon layer formed over the irradiated region is more than the ion range. For doses higher than $2 \times 10^{12} \text{ cm}^{-2}$, the etch rate of the irradiated regions is much slower than the unirradiated regions, so that some parts of the structure still remains as the isotropic process continue to undercut the structure. This explains the

non-uniform light emission from the squares irradiated with 5×10^{12} and 10^{13} cm^{-2} . When the dose is large enough, no porous silicon is formed in the irradiated regions, resulting in no PL emission. The structure height would then correspond to the range of 2 MeV He which is $7.2 \mu\text{m}$. A plot of the thickness, t , of porous silicon layer versus dose is shown in Fig. 5(b). The rate of porous silicon formation reduces rapidly as the dose increase from 10^{12} to 10^{13} cm^{-2} .

Fig. 6 shows a graphic demonstration of the ability to create multi-colour emission by variable dose irradiation. Using the *Ionscan* software, 13 circles were irradiated each of equal dose irradiation but with the radius decreasing to the centre, over the same spot. This means that the dose increases linearly from the border to the centre of the circle. Fig. 6(a) shows the concentric circle irradiated with doses ranging from 1×10^{12} to $1.3 \times 10^{13} \text{ cm}^{-2}$. This dose range corresponds to the emission wavelength from green to red, indicated in Fig. 3. This resulted in a concentric

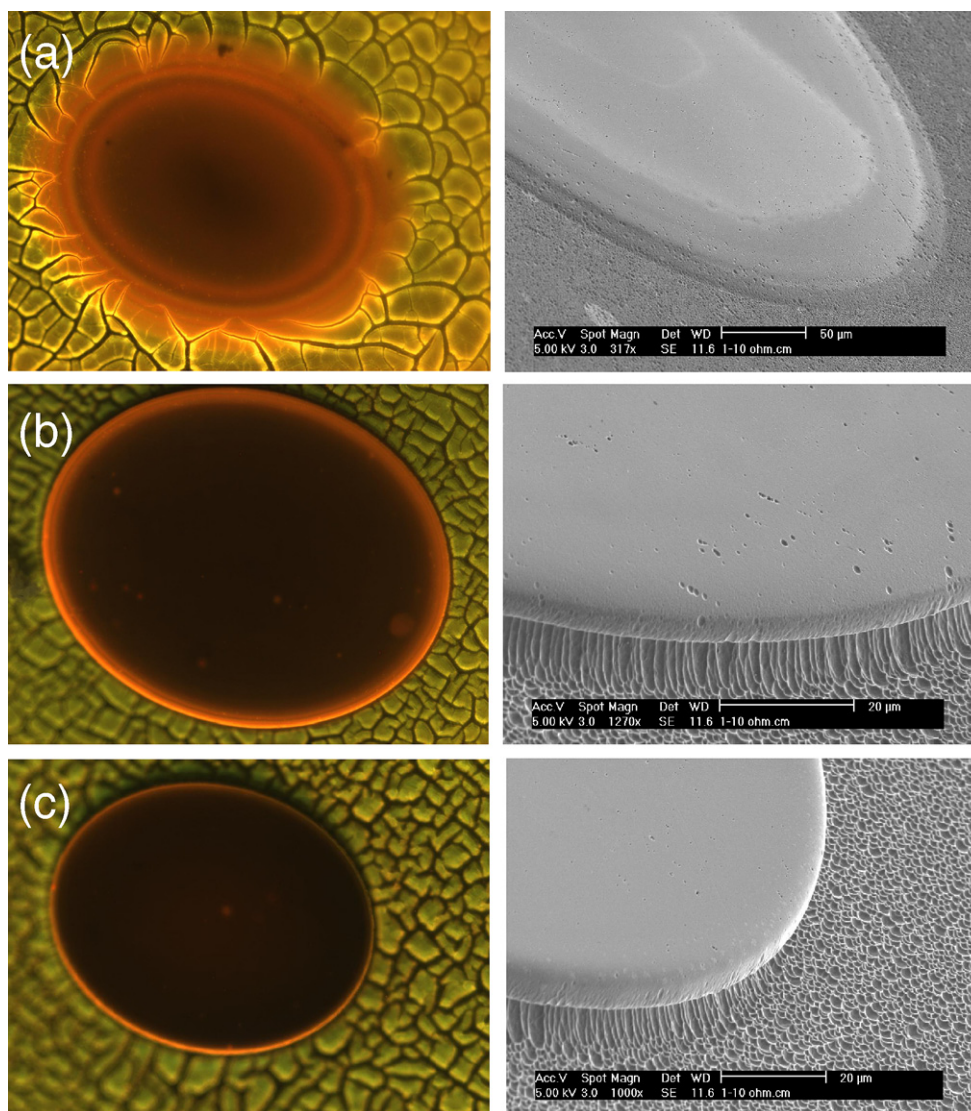


Fig. 6. (Colour online) Concentric circles irradiated with dose from (a) 1×10^{12} to 1.3×10^{13} , (b) 1×10^{13} to 1.3×10^{14} and (c) 1×10^{14} to $1.3 \times 10^{15} \text{ cm}^{-2}$. Dose increases linearly from outer to inner ring over 13 circles.

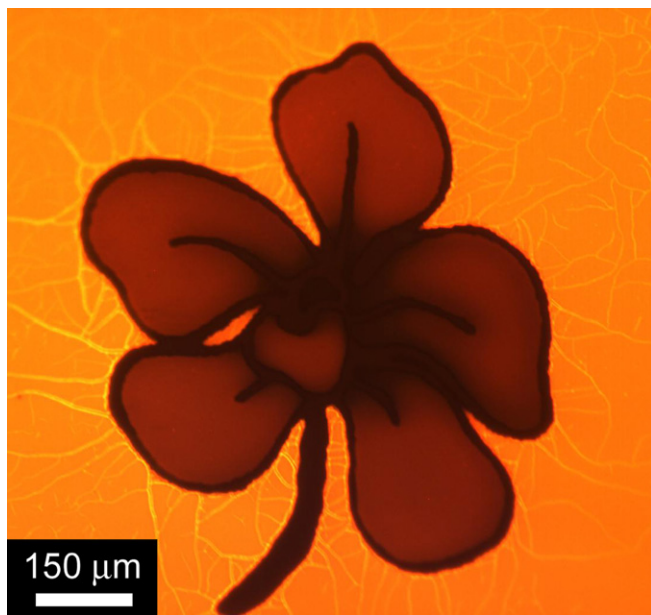


Fig. 7. (Colour online) A $700 \times 700 \mu\text{m}$ PL image of an orchid created in porous silicon.

pattern whereby the wavelength shifts gradually from green on the border to red at the centre. Figs. 6(b) and (c) show similar concentric patterns but irradiated with higher dose ranges. In both cases, no light is emitted from the patterns, as the large dose inhibits porous silicon from forming in the irradiated regions. Near the edges of the circle, we can still see a red rim as the etch rate tends to be faster at the sides [15].

This technique also allows us to irradiate any arbitrary patterns and shapes directly into the sample. A figure of the orchid flower was patterned into silicon with a dose of $2 \times 10^{12} \text{ cm}^{-2}$. Fig. 7 shows a $700 \times 700 \mu\text{m}$ PL image of the red orchid on a yellow background after keeping the sample for 15 days in the sealed chamber. The black outline of the flower was created by using a high dose irradiation.

4. Conclusions

In conclusion, we have demonstrated the use of accurately controlled doses of high energy helium ion irradiation for tuning the light emission of porous silicon with sub-micron spatial resolution. The wavelength emission is red-shifted from 590 to 650 nm as dose increases from

5×10^{11} to $1 \times 10^{13} \text{ cm}^{-2}$. The PL intensity is quenched for doses higher than 10^{13} cm^{-2} as porous silicon inhibited from forming at the irradiated regions. This technique has opened up new research opportunities of fabricating silicon-based light emitting devices and displays for optoelectronics applications.

References

- [1] L.T. Canham, *Appl. Phys. Lett.* 57 (1990) 1046.
- [2] V. Lehmann (Ed.), *Electrochemistry of Silicon*, Wiley-VCH, Weinheim, 2002.
- [3] A.J. Kontkiewicz, A.M. Kontkiewicz, J. Siejka, S. Sen, G. Nowak, A.M. Hoff, P. Sakthivel, K. Ahmed, P. Mukherjee, S. Witanachchi, J. Lagowski, *Appl. Phys. Lett.* 65 (1994) 1436.
- [4] H. Mizuno, H. Koyama, N. Koshida, *Appl. Phys. Lett.* 69 (1996) 3779.
- [5] M.V. Wolkin, J. Jorne, P.M. Fauchet, G. Allan, C. Delerue, *Phys. Rev. Lett.* 82 (1999) 197.
- [6] V.V. Doan, M.J. Sailor, *Science* 256 (1992) 1791.
- [7] S.P. Duttgupta, C. Peng, P.M. Fauchet, S.K. Kurinec, T.N. Blanton, *J. Vac. Sci. Technol. B* 13 (1995) 1230.
- [8] M. Rocchia, S. Borini, A.M. Rossi, L. Boarino, G. Amato, *Adv. Mater.* 15 (2003) 1465.
- [9] D.J. Sirbulu, G.M. Lowman, B. Scott, G.D. Stucky, S.K. Buratto, *Adv. Mater.* 15 (2003) 149.
- [10] X.M. Bao, H.Q. Yang, F. Yan, *J. Appl. Phys.* 79 (1993) 1320.
- [11] L. Pavesi, G. Giebel, F. Ziglio, G. Mariotto, F. Priolo, S.U. Campisano, C. Spinella, *Appl. Phys. Lett.* 65 (1994) 2182.
- [12] F. Watt, J.A. van Kan, A.A. Bettiol, T.F. Choo, M.B.H. Breese, T. Osipowicz, *Nucl. Instr. and Meth. B* 210 (2003) 14.
- [13] P. Polesello, C. Manfredotti, F. Fizzotti, R. Lu, E. Vittone, G. Lerondel, A.M. Rossi, G. Amato, L. Boarino, S. Galassini, M. Jaksic, Z. Pastuovic, *Nucl. Instr. and Meth. B* 158 (1999) 173.
- [14] E.J. Teo, M.B.H. Breese, E.P. Tavernier, A.A. Bettiol, F. Watt, M.H. Liu, D.J. Blackwood, *Appl. Phys. Lett.* 84 (2004) 3202.
- [15] M.B.H. Breese, F.J.T. Champeaux, E.J. Teo, A.A. Bettiol, D.J. Blackwood, *Phys. Rev. B* 73 (2006) 035428.
- [16] P. Mistry, I. Gomez-Morilla, G.W. Grime, R.P. Webb, R. Gwilliam, A. Cansell, M. Merchant, K.J. Kirkby, E.J. Teo, M.B.H. Breese, A.A. Bettiol, D.J. Blackwood, F. Watt, *Nucl. Instr. and Meth. B* 237 (2005) 188.
- [17] E.J. Teo, M.B.H. Breese, A.A. Bettiol, D. Mangaiyarkarasi, F.J.T. Champeaux, F. Watt, D.J. Blackwood, *Adv. Mater.* 18 (2006) 51.
- [18] E.J. Teo, D. Mangaiyarkarasi, M.B.H. Breese, A.A. Bettiol, D.J. Blackwood, *Appl. Phys. Lett.* 85 (2004) 4370.
- [19] D. Mangaiyarkarasi, E.J. Teo, M.B.H. Breese, A.A. Bettiol, D.J. Blackwood, *J. Electrochem. Soc.* 152 (2005) D173.
- [20] J.A. van Kan, A.A. Bettiol, F. Watt, *Appl. Phys. Lett.* 83 (2003) 1629.
- [21] A.A. Bettiol, C.N.B. Udalagama, J.A. van Kan, F. Watt, *Nucl. Instr. and Meth. B* 231 (2005) 400.
- [22] M.B.H. Breese, P.J.C. King, G.W. Grime, F. Watt, *J. Appl. Phys.* 72 (1992) 2097.
- [23] M.B.H. Breese, G.W. Grime, M. Dellith, *Nucl. Instr. and Meth. B* 77 (1993) 332.